# Atypical molecular basis for drug resistance to mitochondrial function inhibitors in *Plasmodium falciparum*

Heather J. Painter[1,a], Joanne M. Morrisey[2], Michael W. Mather[2], Lindsey M. Orchard[1], Cuyler Luck[1], Martin J. Smilkstein[3], Michael K. Riscoe[3], Akhil B. Vaidya[2], Manuel Llinás[1]

[1] Department of Biochemistry and Molecular Biology, Huck Center for Malaria Research, Pennsylvania State University, University Park, PA, USA

[2] Center for Molecular Parasitology, Department of Microbiology and Immunology, Drexel University College of Medicine, Philadelphia, PA, USA

[4] Medical Research Service, Department of Veterans Affairs Medical Center, Portland, OR, USA

[a] Current affiliation: United States Food & Drug Administration, Center for Biologics & Evaluation Research, Office of Vaccine Research & Review, Division of Parasites, Bacteria & Allergenic Products, Silver Spring, MD, USA

[#] Corresponding authors: manuel@psu.edu and Heather.Painter@fda.hhs.gov

**Abstract:**

The continued emergence of drug-resistant *Plasmodium falciparum* parasites hinders global attempts to eradicate malaria, emphasizing the need to identify new antimalarial drugs. Attractive targets for chemotherapeutic intervention are the cytochrome (cyt) $bc_1$ complex, which is an essential component of the mitochondrial electron transport chain (mtETC) necessary for ubiquinone recycling and mitochondrially localized dihydroorotate dehydrogenase (DHODH) critical for *de novo* pyrimidine synthesis. Despite the essentiality of this complex, resistance to a novel acridone class of compounds targeting cyt $bc_1$ was readily attained, resulting in a parasite strain (SB1-A6) that was pan-resistant to both mtETC and DHODH inhibitors. Here we describe the molecular mechanism behind the resistance of the SB1-A6 parasite line which lacks the common cyt $bc_1$ point mutations characteristic of resistance to mtETC inhibitors. Using Illumina whole-genome sequencing, we have identified both a copy number variation (~2x) and a single-nucleotide polymorphism (C276F) associated with *pfdhodh* in SB1-A6. We have characterized the role of both genetic lesions by mimicking the copy number variation via episomal expression of *pfdhodh* and introducing the identified SNP using CRISPR/Cas9 and assessed their contributions to drug resistance. Although both of these genetic polymorphisms have been previously identified as contributing to both DSM-1 (1) and atovaquone resistance (2, 3), SB1-A6 represents a unique genotype in which both alterations are present in a single line, suggesting that the combination contributes to the pan-resistant phenotype. This novel mechanism of resistance to mtETC inhibition has critical implications for the development of future drugs targeting the $bc_1$ complex or *de novo* pyrimidine synthesis that could help guide future anti-malarial combination therapies and reduce the rapid development of drug resistance in the field.

43 **Introduction:**

44 Infection by the human malaria parasite *Plasmodium falciparum* rapidly leads to the clinical
45 symptoms associated with the 48-hour asexual replicative cycle of the parasite within the blood of
46 the host (4). *P. falciparum* malaria continues to present an enormous global public health burden
47 due to the lack of an effective long-term vaccine (5) and the emergence of resistance to front-line
48 antimalarial chemotherapies (6). This underscores the continued need to maintain a robust drug
49 development pipeline that produces novel and effective antimalarial compounds for future
50 deployment.

51 To accelerate novel anti-malarial compound identification, independent laboratories and global
52 consortia have rapidly identified numerous chemical entities that are efficacious against multiple
53 *Plasmodium* species and developmental stages. Despite the diverse chemical scaffolds in the
54 compounds tested, most effective candidates tend to have similar modes-of-action in the malaria
55 parasite due to the paucity of molecular targets that are significantly divergent from the human
56 host (7-9). As such, it is not surprising that a large and diverse set of compounds selectively target
57 the highly divergent *Plasmodium* mitochondrion (7), which is essential for *de novo* pyrimidine
58 synthesis during the blood stages of parasite development (10, 11).

59 Although the *Plasmodium* mitochondrion maintains the canonical tricarboxylic acid cycle pathway
60 of central carbon metabolism (12-15), these enzymes are dispensable for blood-stage development
61 (15). We have previously shown the main role of the parasite mitochondrion during the blood-
62 stage is the provision of precursors for *de novo* pyrimidine synthesis (10), a process requiring a
63 ubiquinone-dependent, mitochondrional dihydroorotate dehydrogenase (DHODH,
64 PF3D7_0603300) and a functioning electron transport chain (ETC) to maintain turnover of

65 ubiquinol, regenerating ubiquinone. This sole essential function of the mitochondrion was
66 established by genetic supplementation with an alternative DHODH from *S. cerevisiae*
67 (yDHODH), which is localized to the cytoplasm and utilizes fumarate as an electron acceptor
68 rather than ubiquinone (10). Therefore, parasites expressing yDHODH from an episome,
69 bypassing the mitochondrially localized PfDHODH, are highly resistant to all chemical inhibitors
70 of the mtETC. Interestingly, the addition of the biguanide prodrug proguanil, combined with the
71 mtETC cytochrome *b* inhibitor atovaquone in the antimalarial drug Malarone, reversed the pan-
72 resistant phenotype of yDHODH expressing *P. falciparum* strain D10 (D10::yDHODH) (10).
73 Although the mode-of-action of atovaquone, as well as other mtETC inhibitors, is well-understood,
74 the molecular target of proguanil remains unknown.

75 Due to the efficacy of disrupting mitochondrial function in the malaria parasite as a strategy for
76 chemotherapeutic intervention, these pathways are the focus of comprehensive anti-mitochondrial
77 drug development programs, and significant efforts have been made to identify novel compounds
78 that target the mtETC both directly (cytochrome *b*) and indirectly (DHODH). To this end, there
79 are several antimalarials, some of which are in the advanced stages of clinical trials, whose
80 proposed modes-of action include interaction with the ubiquinone binding pocket(s) of DHODH
81 (DSM-1 and DSM265) (16-18) or cytochrome *b* (ELQ-300 and 6-$NH_2$Ac) (19, 20). Despite the
82 essentiality of both components of the mtETC, resistance to these compounds readily arose and
83 genotyping of resistant parasites revealed either amplification of or point mutations in DHODH,
84 as well as point mutations within cytochrome *b* (1, 2, 16, 21-23). However, parasites resistant to
85 6-$NH_2$Ac, an acridone compound thought to target the mtETC $bc_1$ complex (20), did not exhibit
86 traditional $bc_1$ resistance mutations (21). The acridone-resistant parasite line SB1-A6 was not only
87 resistant to 6-$NH_2$Ac but also exhibited pan-resistance to all mitochondrial inhibitors to which the

88 parent strain, D6, was susceptible (21). Again, this resistance was abrogated by the addition of
89 proguanil (21), similar to *P. falciparum* parasites that express yDHODH, and confirming the target
90 of acridones to be the *P. falciparum* mtETC, although the provenance of the phenotypic similarities
91 in resistance to $bc_1$ complex inhibitors between SB1-A6 and the yDHODH transgenic parasite line
92 was unclear (10).

93 In this study, we present a clear genotype for the *P. falciparum* SB1-A6 acridone-resistant clonal
94 parasite strain and, through a combination of targeted and whole-cell methods, establish that the
95 mechanism of resistance to both cytochrome $bc_1$ and DHODH inhibitors results from the
96 contribution of multiple genetic polymorphisms. We find that *P. falciparum* SB1-A6 accumulates
97 both a copy number variation and a specific mutation in PfDHODH, and both of these genetic
98 polymorphisms contribute to the pan-resistant phenotype. This study uncovers a mechanism of
99 cross-resistance between PfDHODH and mtETC inhibitors and serves as a cautionary note to
100 future anti-malarial combination therapy formulations containing such drugs.

101

102 **Results:**

103 **Strain SB1-A6 displays pan-resistance to mtETC inhibitors.**

104 To confirm the resistance phenotype of *P. falciparum* SB1-A6 (21) and the line's similarity to *P.*
105 *falciparum* D10::yDHODH (10), we first tested the susceptibility of both strains to the classic
106 malaria parasite cytochrome $bc_1$ inhibitor, atovaquone, using a growth inhibition assay (Fig. 1A,
107 Table S1). As expected, both SB1-A6 and D10::yDHODH displayed resistance to atovaquone,
108 while the parental strains (D6 and D10, respectively) were susceptible (Fig. 1A. Table S1), as
109 previously published (21). It has been well established that expression of yDHODH in *P.*

110 *falciparum* results in resistance to the PfDHODH inhibitor DSM-1 (24, 25). Therefore, we tested
111 the susceptibility of SB1-A6 to direct inhibition of PfDHODH with DSM-1 (17) and found that
112 this parasite line was resistant to both DHODH, as well as cytochrome $bc_1$ inhibitors (Figure 1B,
113 Table S1), making it the first *P. falciparum* clone generated to exhibit such cross-resistance (21).
114 However, more recent studies aimed at generating resistance to atovaquone by increasing drug
115 concentration exposure step-wise have also resulted in cross-resistance to DSM-1 (2). Resistance
116 to mtETC inhibitors due to an alternative source of pyrimidines is abolished by the addition of the
117 prodrug proguanil (10). Likewise, resistance to atovaquone inhibition of the mtETC in SB1-A6
118 was reversed upon the addition of 1.5µM proguanil (Fig. 1B, Table S1), suggesting that the
119 mechanism of pan-resistance to mitochondrial inhibitors is linked to the function of PfDHODH,
120 as was previously demonstrated for D10::yDHODH (10).

121 Drug resistance mechanisms in both prokaryotes and eukaryotes can involve "rewiring" to
122 overcome the inhibition of essential metabolic pathways by genetic variation, metabolic bypass,
123 or efflux mechanisms. Metabolomics has become a useful tool for unraveling anti-parasite drug
124 mechanisms of action and resistance (8, 26, 27). To elucidate the mechanism(s) of resistance in
125 SB1-A6, we determined if any metabolic perturbations occurred in the SB1-A6 drug-resistant line
126 due to drug treatment that could account for cross-resistance to both PfDHODH and cytochrome
127 $bc_1$ inhibition, using whole-cell metabolomics analysis. Trophozoite-stage D6 and SB1-A6 were
128 exposed to ~10x IC50 of either atovaquone (10nM) or DSM-1 (1.5µM) for 2 hours, followed by
129 whole-cell metabolite extraction, and quantitated by LC-MS/MS analysis (8). Metabolomic
130 analysis showed that treatment of SB1-A6 with DSM-1 or atovaquone did not result in any
131 significant metabolic perturbation (Fig. 1C and 1D; Table S1), whereas treatment of the wild-type
132 D6 revealed an accumulation of *de novo* pyrimidine synthesis precursors compared to an untreated

133 control (Fig 1C and 1D). The accumulation of pyrimidine precursors in the parental line upon
134 treatment with either atovaquone or DSM-1 and lack of accumulation in the treated mutant line
135 (Fig. 1D), in neither a stage- nor time-dependent manner (Fig. S1) is consistent with the
136 involvement of DHODH in the mechanism of resistance.

137 **Genetic determinants of pan-resistance to mtETC and pyrimidine synthesis inhibition in**
138 **SB1-A6.**

139 Previous studies have demonstrated that genetic mechanisms of resistance resulting in the ability
140 of the parasite to overcome mtETC and *de novo* pyrimidine synthesis inhibition include mutations
141 in either *cytochrome b* (28, 29) or *pfdhodh* (1, 30) or copy number variation of *pfdhodh* (2, 3).
142 Analysis of the SB1-A6 *cytochrome b* sequence by Smilkstein *et al.* (21) did not reveal any
143 mutations. Therefore, to identify any genetic polymorphisms that could lead to a molecular
144 mechanism of resistance, we examined the genomes of both the D6 wild-type and SB1-A6 drug-
145 resistant parasites using Illumina-based next-generation DNA sequencing. Whole-genome
146 sequencing revealed a non-synonymous G → T point-mutation in the coding sequence of
147 PfDHODH, resulting in the amino acid change C276F (Fig. 2A, Table S2). Amino acid C276 is
148 localized adjacent to the flavin mononucleotide binding pocket (Fig. 2C), and the substitution to a
149 phenylalanine has been demonstrated to reduce the size of the binding pocket where DSM-1 binds
150 (1), resulting in a binding pocket structure resembling that of HsDHODH (30). Although this
151 mutation was not the only change found in SB1-A6 (Table S2), it was the only change in an
152 annotated gene known to be directly linked to pyrimidine synthesis and/or mitochondrial function.

153 In addition, we identified a ~20kb, 2-fold copy number variation (CNV) in the SB1-A6 genome,
154 including the coding sequence for PfDHODH, as well as six other protein-coding genes (Fig. 2B).
155 We further confirmed the presence of this copy number increase by DNA microarray comparative

156 genome hybridization (Table S3). This region has previously been shown to increase in copy
157 number in *P. falciparum* selected for resistance to DSM-1 (3), resulting in cross-resistance to
158 atovaquone (2). Although each of these genetic polymorphisms has individually been previously
159 identified as contributing significantly to both DSM-1 (1) and atovaquone resistance (2, 3), SB1-
160 A6 possesses a unique genotype in which both alterations are present in a single parasite line,
161 suggesting that the combination contributes to the pan-resistant phenotype of this line.
162 Intriguingly, the increased CNV of PfDHODH did not directly translate to higher protein levels
163 (Fig. 2D), nor did it produce any obvious mislocalization (Fig. S2) of the protein in the parasite.

164 Due to previous observations that linked the PfDHODH C276F mutation and CNV to both DSM-
165 1 and atovaquone resistance, respectively (2, 3), we examined the function of PfDHODH in
166 mitochondria isolated from D6 and SB1-A6 to determine if these polymorphisms could account
167 for the reduced sensitivity of SB1-A6 parasites to mitochondrial inhibition. Measurement of
168 DHODH activity in isolated mitochondria from trophozoite stages of D6 and SB1-A6 revealed
169 that the enzymes of both strains are equally susceptible to inhibition by DSM-1 (Fig. 2E),
170 confirming the results from purified wild-type and C276F mutant PfDHODH activity assays (1).
171 Interestingly, measurement of the specific activity of DHODH from SB1-A6 isolated mitochondria
172 revealed a two-fold increase compared to D6 (Fig. 2F), possibly due to the increase in copy number
173 of PfDHODH. Although the C276F mutation does not lead to a decrease in the ability of DSM-1
174 to inhibit PfDHODH, these data suggest that the SB1-A6 parasite line has gained the ability to
175 withstand either mtETC or pyrimidine biosynthesis inhibition by increasing the overall activity of
176 PfDHODH allowing sufficient levels of nucleotide synthesis for parasite survival.

177 **Genetic supplementation of DHODH increase copy number and CRISPR-Cas9 introduction**
178 **of C276F point mutation**

179 Previous studies have established that *P. falciparum* grown in the presence of step-wise increasing
180 concentrations of DSM-1 leads to an increase in copy number of a chromosomal region that
181 includes PfDHODH leading to resistance to both DSM-1 (3) and atovaquone (2). To test the
182 hypothesis that a copy number increase in PfDHODH also results in decreased sensitivity of SB1-
183 A6 parasites to inhibition of electron transport or *de novo* pyrimidine synthesis, we introduced
184 either wild-type or mutant (C276F) PfDHODH expressed from an episomal vector under the
185 control of a constitutive promoter in the drug-susceptible strain D6 (Fig. 3A). After selection of a
186 parasite population containing the mutant or wild-type PfDHODH, we assessed the susceptibility
187 of these parasites to atovaquone or DSM-1 using a standard growth inhibition assay. The
188 introduction of additional copies of PfDHODH resulted in decreased susceptibility to DSM-1 and
189 atovaquone (Fig. 3B). Notably, the episomal expression of the mutant PfDHODH also results in
190 almost complete resistance to atovaquone (Fig. 3B), phenocopying the genotype of SB1-A6.
191 Episomal increase of wild-type PfDHODH results in a ten to 100-fold decrease in susceptibility to
192 DSM-1 (Fig. 3B), confirming the phenotype established by Guler *et al.* of DSM-1 and atovaquone
193 resistant parasites with an increased copy number of PfDHODH (2, 3).

194 Since the discovery that *P. falciparum* survival is dependent upon *de novo* pyrimidine synthesis
195 (10), PfDHODH has become a popular target for chemical intervention strategies (17, 18, 31, 32).
196 For example, discovery efforts have led to the development of triazolopyrimidine-based inhibitors
197 for PfDHODH, which are currently undergoing clinical trials for safety and efficacy (16, 33). *In*
198 *vitro* selection of *P. falciparum* for resistance to compound DSM265 led to the identification of
199 various mutations within PfDHODH (1). Of these mutations, C276F was determined to reduce
200 the binding capacity of chemical inhibitors using in an *in vitro* expression system (1), as well as
201 computational docking studies (30). To test the hypothesis that the same observed point mutation

202 in SB1-A6 PfDHODH contributes to *P. falciparum* resistance to both PfDHODH and cytochrome
203 $bc_1$ inhibitors, we utilized CRISPR/Cas9 (34) to genetically introduce the C276F mutations into
204 this gene in D6 and also repair it in SB1-A6 (Fig. 3C; Fig S3A and S3B). After confirming the
205 introduction or repair of the mutation at amino acid 276 (Fig. S3A and S3B), we then performed
206 drug susceptibility assays to quantitate the contribution of this mutation to the pan-resistant
207 phenotype (Table S1). While we were able to reverse this mutation to the wild-type background
208 in $A6^{F276C}$ decreasing the overall resistance to both atovaquone and DSM-1 (Fig. 3D, Table S1),
209 there remains an increased CNV of PfDHODH, which is likely contributing to the higher IC50
210 than demonstrated for D6 (Fig. 3D; Table S1). Conversely, susceptibility to atovaquone is only
211 decreased by 2-fold due to the introduction of C276F into strain D6 (Fig. 3D; Table S1).
212 Interestingly, these assays show that this mutation results in a 10-fold increase in the IC50 of DSM-
213 1 in $D6^{C276F}$ (Fig. 3D) and a 40-fold decrease in $A6^{F276C}$ (Fig. 3D). These results suggest that the
214 point mutation directly contributes to decreased efficacy of direct inhibition of PfDHODH and
215 enhances the ability of *P. falciparum* to overcome mtETC inhibition (Table S1). Taken together,
216 these data demonstrate the coordination between genetic polymorphisms of the PfDHODH SNP
217 and CNV in the SB1-A6 parasite line that mediates the pan-resistance phenotype.

218 **Discussion:**

219 In this study, we have demonstrated the coordination of two genetic polymorphisms that result in
220 resistance to compounds that target the mtETC. First, the copy number increase of DHODH results
221 in the reduced susceptibility to $bc_1$ complex and *de novo* pyrimidine synthesis inhibition.
222 However, a two-fold increase in DHODH, by itself, was not sufficient for complete resistance to
223 mtETC inhibitors, potentially due to a reliance on other genes within the CNV amplicon. Aside
224 from DHODH, this amplicon encompasses seven genes, a majority of which are unannotated,

225 except for PF3D7_0603200 (*bcs1*: mitochondrial chaperone, putative) and PF3D7_0602800 (*jmjc*:
226 jumanji-C demethylase domain containing), the gene products of which could contribute to the
227 drug-resistant phenotype. This is supported by previous studies that demonstrated that a similar
228 amplicon results in resistance to both atovaquone and DSM-1 (2, 3). Further work is necessary to
229 determine if the proteins encoded for on the amplicon are involved in reducing the parasite's
230 susceptibility to mtETC and *de novo* pyrimidine synthesis inhibition.

231 The implications of the SB1-A6 phenotype should be emphasized in considerations of the mtETC-
232 pyrimidine-biosynthesis axis as an anti-malarial drug target. While the adaptation that led to SB1-
233 A6 seems to have been a unique event, both the CNV and C276F point mutations have each been
234 derived independently from exposure to atovaquone and DSM-256, a next-generation PfDHODH
235 inhibitor currently in clinical trials. Therefore, the possibility that adaptations similar to those
236 found in SB1-A6 may arise during clinical trials or deployment of new $bc_1$ complex or DHODH
237 inhibitors deserves consideration. While concerns regarding atovaquone resistant mutations in the
238 *cytb* gene on mtDNA have been largely allayed due to lack of inheritance during transmission
239 within the mosquito vector (35), we have no reason to discount the transmissibility of nuclear-
240 encoded *pfdhodh* polymorphisms at present. Since these adaptations can be overcome by the
241 addition of proguanil, the continued inclusion of proguanil or an effective replacement should be
242 considered in future combinations. In addition to the question of transmissibility and choice of
243 partner drugs, the ultimate significance of the SB1-A6 phenotype to future anti-malaria drug
244 choices may also differ between treatment use and prophylaxis. During treatment parasite number
245 is high, increasing the risk for selection of both pre-existing and *de novo* resistant parasites,
246 whereas, in causal prophylactic use, in the absence of pre-existing resistance the risk would be

247 expected to be negligible. In either case, assessing the risk and monitoring for the emergence of
248 the SB1-A6 phenotype should be done.

249 This study presents the first identification of the acquisition of multiple genetic polymorphisms in
250 response to a $bc_1$ complex inhibitor that results in pan-resistance to both direct and indirect
251 inhibitors of DHODH. Fully elucidating the molecular mechanisms of this pan-resistance is
252 essential to inform future chemotherapeutic targeting strategies for malaria elimination. The
253 emergence of resistance to many of the drugs in the antimalarial arsenal has highlighted the
254 urgency of developing future medicines with modes of action distinct to those of the current
255 therapies. More recently, considerations have been made for combination therapies that target a
256 single essential metabolic pathway via different modes-of-action. In light of the potential
257 development of cross-resistance to a single inhibitor due to its combinatorial partner, the molecular
258 mechanisms of resistance for future therapeutic strategies should be thoroughly investigated prior
259 to approval for use in the clinical setting.

260 Recently, the essentiality of DHODH has been demonstrated in cell-cycle arrested cancer cells
261 without mitochondria wherein reactivation of growth occurs upon the acquisition of mtETC-linked
262 DHODH (36), suggesting that the lack of de novo pyrimidine synthesis is a major obstacle for in
263 vivo growth of respiration-compromised tumor cells. The combined detrimental effects of both
264 dysfunctional mitochondrial respiration and mtETC-linked de novo pyrimidine synthesis on cell
265 growth strengthen their relevance as drug targets against both parasite development and
266 metastatic cell growth. This further emphasizes the continued benefit of identifying novel
267 inhibitors of DHODH that could ultimately be appropriated for both parasite elimination and
268 perhaps extended to treatment targeting metastatic cells within the human host.

269

270 **Methods:**

271 ***Parasite Strains and Culture:*** *Plasmodium falciparum* strains D6 and SB1-A6 were provided by
272 Michael Riscoe and Martin Smilkstein (21). All parasites obtained from other sources or generated
273 in this study were maintained under standard conditions (37) at 2% hematocrit with O+ human
274 erythrocytes in RPMI1640 (Thermo Fisher Scientific) containing hypoxanthine, $NaH_2CO_3$
275 (Sigma-Aldrich), HEPES (Sigma-Aldrich), glutamine (Sigma-Aldrich) and 2.5 g/L AlbuMAX II
276 (Thermo Fisher Scientific). Intraerythrocytic developing parasites were synchronized with 5%
277 sorbitol (Sigma-Aldrich) over three subsequent developmental cycles to synchronize parasites
278 within 4-6 hours, as previously described (38).

279 Parasite cultures were maintained Mycoplasma-free and were confirmed prior to metabolomic
280 analysis. Separate mycoplasma-free culture apparatus and solutions were used for all
281 metabolomics culturing to prevent contamination. Cultures were checked for mycoplasma
282 contamination weekly using IntronBio *e*-Myco™, Mycoplasma PCR Detection kit (Boca
283 Scientific; cat. no. 25235). If parasite cultures tested positive for Mycoplasma, cultures were
284 treated as per manufacturer's instructions with Mycoplasma Removal Agent (MP Biomedicals,
285 LLC.; cat. no. 30-500-44).

286

287 ***Drug Inhibition Assays:*** All parasite growth inhibition assays were performed in 96-well plates
288 as described by Desjardin *et al.* (39) and adapted for SYBR Green I (40). Drugs were prepared in
289 DMSO as a 500× dilution series (typically a 2- or 3-fold dilution series was used, yielding a final
290 concentration in media ranging from 0.001−30 μM depending on the cell line) and were then
291 diluted 1:50 into media to yield a final DMSO concentration of 0.2%. Parasites were diluted to 1%

292 parasitemia and 1% hematocrit in each well of a 96-well plate then propagated for 48 h and growth
293 was assessed using the SYBR Green method. SYBR green fluorescence was measured (ex./em.
294 485/535 nm) and data analysis was performed using GraphPad Prism 7. For transgenic *P.*
295 *falciparum* strains generated in this study, parasites were propagated for three intraerythrocytic
296 cycles in media lacking drug before plating. All data were collected in triplicate and biological
297 duplicate.

298

299 ***Mitochondrial Activity Assays:*** *P. falciparum* cultures were synchronized at least twice by
300 treatment with alanine (41), expanded and harvested at 8-15% parasitemia in the mid to late
301 trophozoite stages. A hemozoin-depleted mitochondrial fraction was isolated from the parasites
302 using nitrogen cavitation, magnetic separation, and differential centrifugation, as previously
303 described (42).

304 DHODH activity assays were conducted essentially as previously described (18, 42) with minor
305 modifications, utilizing the ubiquinone analog decylubiquinone as the primary electron acceptor,
306 coupled to the redox dye 2,6-dichloroindophenol to take advantage of the latter's higher extinction
307 coefficient and absorbance in the visible range. Assays contained 1 mM L-dihydroorotate, 100 µM
308 decylubiquinone, 60 µM 2,6-dichloroindophenol, 50 mM sodium malonate, 2 mM potassium
309 cyanide, 100 mM potassium chloride, 0.05% Triton X-100, 10 % glycerol, and 0.1 M HEPES (pH
310 7.6) in a final volume of 1 ml. 5 ul aliquots of diluted inhibitor or vehicle (DMSO) was added, and
311 each assay was initiated by addition of a 7 µl aliquot of mitochondrial preparation (50-110 µg
312 protein) and recorded with a modified SLM-AMINCO DW2C dual-wavelength
313 spectrophotometer (On-Line Instrument Systems, Inc., Bogart, GA, USA) in dual mode (600 nm
314 – 528 nm) at 30°C.

315

316 ***Inhibitors:*** The antimalaria compound atovaquone was a gift from Glaxo Wellcome, Research
317 Triangle Park, N.C. Proguanil was kindly provided by the Jacobus Pharmaceutical Company,
318 Princeton, NJ, USA. Both ELQ-300 and 6-NH2Ac were contributed to this study by Michael
319 Riscoe, Oregon Health Sciences University, Portland, OR, USA. DSM-1 (17) and DSM-265 (16)
320 were provided by Margaret Phillips, University of Texas Southwestern, Dallas, TX, USA.
321 Chloroquine (Cat# C6628) was purchased from Sigma-Aldrich, St. Louis, MO, USA.

322

323 ***Whole-cell Metabolomics:*** Metabolite extractions, data collection, and analysis were performed
324 as described previously (8, 43, 44). Briefly, a ~20 µL pellet of cells was resuspended in 1 mL of
325 pre-chilled 90:10 methanol:water and placed at 4˚C. The internal standard $^{13}C_4$-$^{15}N_1$-aspartate was
326 spiked into the extraction methanol solution to control for sample preparation and handling.
327 Samples were vortexed, resuspended, and centrifuged for 10 min at 15000 RPM and 4˚C.
328 Supernatants were collected and stored at -80˚C or dried down immediately under nitrogen flow.
329 The dried metabolites were resuspended in HPLC-grade water (Sigma-Aldrich, CHROMASOLV)
330 to between $1x10^5$ and $1x10^6$ cells/µL, based on hemocytometer counts of purified parasites. All
331 samples were processed in technical triplicate with method blanks to reduce unwanted variation
332 and account for background signal, respectively. Samples were randomized and 10µL of
333 resuspended metabolite extract or method blank was injected for ultraHigh-Performance Liquid
334 Chromatography-Mass Spectrometry (HPLC-MS) analysis.

335 Extracts were analyzed using HPLC-MS on a Thermo Exactive Plus Orbitrap™. Metabolite
336 separation was performed with a C18 column (Phenomenex Hydro-RP; cat. No 00D-4387-B0)

337 using a 25 minute gradient of A: 3% aq. methanol/15mM acetic acid/10 mM tributylamine ion-
338 pairing agent and B: 100% MeOH (45). Metabolite detection was performed using a scan range
339 of 85-1000 m/z and a resolution of 140,000 @ m/z 200, in negative ion mode. The detection of
340 cellular metabolites was aided by the generation of a database from 292 pure metabolite standards
341 using the same instrument and method to determine detection capability, mass/charge ratio (m/z),
342 and retention time for each metabolite. Analysis of data was carried out as previously described
343 (8).

344

345 ***Whole-genome Sequencing and Analysis:*** Genomic DNA was isolated, prepared from *P.*
346 *falciparum* parasite lines, and sequenced as previously described (46). Briefly, a total of 10 µg of
347 gDNA from each line was sheared to obtain a fragment size of ~200–400 bp. The resulting sheared
348 gDNA was size selected on a 2% (w/v) low-melting agarose gel and then purified and concentrated
349 using MinElute purification columns followed by the QIAquick PCR purification kit (QIAGEN).
350 Barcoded libraries for Illumina TruSeq single-end sequencing were then constructed from the size-
351 selected, sheared material and size selected using Agencourt AMPure XP magnetic beads
352 (Agencourt Biosciences, Beckman Coulter). The quality of the final sequencing libraries was
353 assessed using an Agilent 2100 Bioanalyzer (Agilent Technologies) and the concentration of each
354 library was quantified using a Quant-iT dsDNA Broad-Range Assay Kit (Invitrogen). The final
355 libraries were multiplexed and 20% (v/v) PhiX control DNA (Illumina, Catalog # FC-110-3001)
356 per lane and were sequenced using an Illumina HiSeq 2500 Rapid Run (150 bp) system (Illumina).

357

358 Sequencing outputs were uploaded into Galaxy (47), which is hosted locally at the Millennium
359 Science Complex at Pennsylvania State University. Sequence reads were mapped to the *P.*
360 *falciparum* 3D7 reference genome v. 10.0 (http://plasmodb.org/common/downloads/release-
361 10.0/Pfalciparum/), using the Burrows-Wheeler alignment tool while selecting and filtering unique
362 reads for Map Quality >30 (48). Sequence variations were detected by Freebayes (version 0.9.0.a)
363 using stringent filtering parameters based on quality and read depth (49, 50). Then SNPeff (version
364 3.3) was applied to annotate and determine the statistical significance of each variant (51). Genome
365 copy number variations were detected based upon local chromosomal read depth using CNVnator
366 (version 0.3) and annotated with Intansv (version 0.99.3) (52).

367

368 ***DHODH Western Blot Analysis:*** Total protein extracts were run on a 4-12% Bis-Tris gel
369 (ThermoFisher) in MES buffer and then transferred to a nitrocellulose membrane. After blocking
370 with 5% milk in PBS-T for 30 minutes, membranes were incubated overnight with the primary
371 antibody in 5% milk. Primary antibodies used were: 1:300 dilution of mouse anti-PfDHODH #3
372 (a kind gift from Margeret Phillips, University of Texas Southwestern) or 1/5000 mouse anti-
373 *Pf*Aldolase-HRP (Abcam, Cat #ab38905). The next day, membranes were washed three times with
374 PBS-T and incubated for two hours with the appropriate secondary antibody, then washed again.
375 The secondary antibody that was used was 1/5,000 goat anti-mouse HRP conjugate (Pierce). ECL
376 reagent (Pierce) was used to detect bound antibody.

377

378 ***DNA Constructs:*** To mutate DHODH using CRISPR-Cas9, complementary oligonucleotides
379 encoding the guide RNA were inserted into pDC2-U6A-hDHFR (kind gift of Marcus Lee) using
380 BbsI sites. A 515 bp homology region containing the mutation in PfDHODH (C276F) or the

381 wildtype sequence from either SB1-A6 or D6 was cloned into StrataClone (Agilent) and then
382 inserted using the NotI site of pDC2-U6A-hDHFR. The resulting plasmids are pDC2-C276F-
383 hDHFR and pDC2-F276C-hDHFR which were co-transfected with Cas9-BSD plasmid from Jose-
384 Juan Lopez-Rubio (34) into D6 and SB1-A6, respectively.
385
386 To introduce multiple copies of either the mutant or wild-type PfDHODH into D6 parasites, *Pf*
387 DHODH was amplified from SB1-A6 (mutant) or D6 (wild-type) genomic DNA including the
388 stop codon, cloned into StrataClone (Agilent), sequence-verified, and then inserted into pLN-
389 ENR-GFP (53) using the AvrII and BsiWI restriction sites. The resulting plasmids, pLN-
390 A6DHODH was transfected into D6 parasites.
391
392 ***Transfection of Plasmodium falciparum.*** Transfection of *P. falciparum* was performed as
393 previously described (54). Briefly, 5-7% ring stage parasite cultures were washed three times with
394 cytomix (55). The parasitized RBC pellet was resuspended to 50% hematocrit in cytomix. The
395 plasmid, isolated using a Qiagen Maxi kit and stored in 50 µg aliquots in ethanol, was centrifuged
396 down and resuspended in 100 µL Cytomix. The plasmid and 250 µL of the 50% parasitized RBC
397 suspension were combined and transferred to a 0.2 cm cuvette on ice. Electroporations were
398 carried out using a BioRad GenePulser set at 0.31kV, 960uF. The electroporated cells were
399 immediately transferred to a T-25 flask containing 0.2 ml uninfected 50% RBCs and 7 mL
400 medium. To select for parasites containing plasmid, medium containing 5 nM WR99210 or 1.5
401 µg/mL Blasticidin was added at 48 hrs post-transfection. Cultures were maintained under constant
402 5 nM WR92210 pressure, splitting weekly, until viable parasites were observed. To confirm the
403 successful mutation of PfDHODH, genomic DNA was purified using the Qiagen DNeasy Blood

404 & Tissue kit and the region of interest was PCR amplified and Sanger sequenced. Positive
405 transfectants were cloned by limiting dilution to obtain a pure population of transgenic parasites.

406

407

408

409 **Author's contributions:**

410 H.P., M.M., J.M., S.C., and C.L. designed and performed experiments and analyzed data. H.P.
411 wrote the manuscript and generated figures. M.M., M.S., and M.R. provided reagents, critical
412 comments, and edits. M.L. and A.V. designed the experiments, provided critical comments, edits,
413 and oversight.

414

415 **Acknowledgments:** We would like to thank the many people who have contributed to this project
416 including Dr. Andrew D. Patterson and Dr. Philip B. Smith of the Penn State Huck Institutes of
417 the Life Sciences Metabolomics Core Facility and Dr. Simon Cobbold previously of the Llinás lab
418 at Princeton University, for analytical expertise, technical oversight; Dr. Craig Praul of the
419 Genomics Core Facility of the Penn State Huck Institutes of the Life Sciences; and the Genomics
420 Core Facility at Princeton University and its staff, especially Donna Storton and Jessica Buckles
421 Wiggins. We also thank Dr. Meg Phillips and Dr. Pradip Rathod for sharing reagents and critical
422 comments. Lastly, we thank the many past and present members of the Llinás lab who supported
423 this project by enhancing the evaluation of data and provided critical comments.

424

**Funding Information:**

This work was supported by generous funding awarded to M.L. from the Bill and Melinda Gates Foundation Grand Challenges Grant (Phase II - OPP1119049), an NIH Director's New Innovators Award (1DP2OD001315-01), the Center for Quantitative Biology (P50 GM071508), and startup funding from the Pennsylvania State University. J.M.M., M.W.M. and A.B.V. were supported by NIH grant R01 AI028398. M.K.R. is a recipient of a VA Research Career Scientist Award (14S-RCS001) and his group receives financial support from the VA's Merit Review Program (i01 BX003312). Research reported in this publication was also supported by the U.S. National Institutes of Health under award number AI100569 (M.K.R., A.B.V., J.M.M., and M.W.M.) and by the U.S. Department of Defense Peer Reviewed Medical Research Program (Log # PR130649; Contract # W81XWH-14-1-0447) (M.K.R.). The team also acknowledges valuable support provided by the Medicines for Malaria Venture. This work was also supported by the Intramural Research Program of the Center for Biologics Evaluation and Research, U.S. Food and Drug Administration funding awarded to H.J.P.

**List of Supplemental Information:**

Supplemental Methods

Table S1: Drug susceptibility assays of various parasite lines

Fig S1: Effects of Inhibitors on pyrimidine synthesis precursors in both sensitive and resistant *P. falciparum.*

Table S2: SNP analysis of the *P.f.* SB1-A6 genome

446 Table S3: Copy number analysis of the *P.f.* SB1-A6 genome

447 Fig S2: IFA of DHODH localization in D6 and SB1-A6

448 Fig S3: Sequence trace of C276F introduction or F276C repair

449

450 **References:**


451 1. White J, Dhingra SK, Deng X, El Mazouni F, Lee MCS, Afanador GA, Lawong A,
452 Tomchick DR, Ng CL, Bath J, Rathod PK, Fidock DA, Phillips MA. 2019. Identification
453 and mechanistic understanding of dihydroorotate dehydrogenase point mutations in
454 *Plasmodium falciparum* that confer in vitro resistance to the clinical candidate DSM265.
455 ACS Infect Dis 5:90-101.
456 2. Guler JL, White J, Phillips MA, Rathod PK. 2015. Atovaquone tolerance in *Plasmodium*
457 *falciparum* parasites selected for high-level resistance to a dihydroorotate dehydrogenase
458 inhibitor. Antimicrob Agents and Chemother 59:686-689.
459 3. Guler JL, Freeman DL, Ahyong V, Patrapuvich R, White J, Gujjar R, Phillips MA, DeRisi
460 J, Rathod PK. 2013. Asexual populations of the human malaria parasite, *Plasmodium*
461 *falciparum,* use a two-step genomic strategy to acquire accurate, beneficial DNA
462 amplifications. PLOS Pathogens 9:e1003375.
463 4. Miller LH, Ackerman HC, Su XZ, Wellems TE. 2013. Malaria biology and disease
464 pathogenesis: Insights for new treatments. Nat Med 19:156-67.
465 5. RTS SCTP. 2015. Efficacy and safety of RTS,S/AS01 malaria vaccine with or without a
466 booster dose in infants and children in Africa: final results of a phase 3, individually
467 randomised, controlled trial. Lancet 386:31-45.
468 6. Cui L, Lindner S, Miao J. 2015. Translational regulation during stage transitions in malaria
469 parasites. Ann N Y Acad Sci 1342:1-9.
470 7. Cowell AN, Istvan ES, Lukens AK, Gomez-Lorenzo MG, Vanaerschot M, Sakata-Kato T,
471 Flannery EL, Magistrado P, Owen E, Abraham M, LaMonte G, Painter HJ, Williams RM,
472 Franco V, Linares M, Arriaga I, Bopp S, Corey VC, Gnadig NF, Coburn-Flynn O, Reimer
473 C, Gupta P, Murithi JM, Moura PA, Fuchs O, Sasaki E, Kim SW, Teng CH, Wang LT,
474 Akidil A, Adjalley S, Willis PA, Siegel D, Tanaseichuk O, Zhong Y, Zhou Y, Llinas M,
475 Ottilie S, Gamo FJ, Lee MCS, Goldberg DE, Fidock DA, Wirth DF, Winzeler EA. 2018.
476 Mapping the malaria parasite druggable genome by using in vitro evolution and
477 chemogenomics. Science 359:191-199.

478 8. Allman EL, Painter HJ, Samra J, Carrasquilla M, Llinas M. 2016. Metabolomic profiling
479 of the malaria box reveals antimalarial target pathways. Antimicrob Agents and Chemother
480 doi:10.1128/AAC.01224-16.
481 9. Cobbold SA, Chua HH, Nijagal B, Creek DJ, Ralph SA, McConville MJ. 2016. Metabolic
482 dysregulation induced in *Plasmodium falciparum* by dihydroartemisinin and other front-
483 line antimalarial drugs. J Infect Dis 213:276-86.
484 10. Painter HJ, Morrisey JM, Mather MW, Vaidya AB. 2007. Specific role of mitochondrial
485 electron transport in blood-stage *Plasmodium falciparum*. Nature 446:88-91.
486 11. Painter HJ, Morrisey JM, Vaidya AB. 2010. Mitochondrial electron transport inhibition
487 and viability of intraerythrocytic *Plasmodium falciparum*. Antimicrob Agents and
488 Chemother 54:5281-7.
489 12. Vaidya AB, Painter HJ, Morrisey JM, Mather MW. 2008. The validity of mitochondrial
490 dehydrogenases as antimalarial drug targets. Trends in Parasitol 24:8-9.
491 13. MacRae JI, Dixon MW, Dearnley MK, Chua HH, Chambers JM, Kenny S, Bottova I,
492 Tilley L, McConville MJ. 2013. Mitochondrial metabolism of sexual and asexual blood
493 stages of the malaria parasite *Plasmodium falciparum*. BMC Biology 11:67.
494 14. Cobbold SA, Vaughan AM, Lewis IA, Painter HJ, Camargo N, Perlman DH, Fishbaugher
495 M, Healer J, Cowman AF, Kappe SH, Llinas M. 2013. Kinetic flux profiling elucidates
496 two independent acetyl-CoA biosynthetic pathways in *Plasmodium falciparum*. J Biol
497 Chem 288:36338-50.
498 15. Ke H, Lewis IA, Morrisey JM, McLean KJ, Ganesan SM, Painter HJ, Mather MW, Jacobs-
499 Lorena M, Llinas M, Vaidya AB. 2015. Genetic investigation of tricarboxylic acid
500 metabolism during the *Plasmodium falciparum* life cycle. Cell Reports 11:164-74.
501 16. Phillips MA, Lotharius J, Marsh K, White J, Dayan A, White KL, Njoroge JW, El Mazouni
502 F, Lao Y, Kokkonda S, Tomchick DR, Deng X, Laird T, Bhatia SN, March S, Ng CL,
503 Fidock DA, Wittlin S, Lafuente-Monasterio M, Benito FJ, Alonso LM, Martinez MS,
504 Jimenez-Diaz MB, Bazaga SF, Angulo-Barturen I, Haselden JN, Louttit J, Cui Y, Sridhar
505 A, Zeeman AM, Kocken C, Sauerwein R, Dechering K, Avery VM, Duffy S, Delves M,
506 Sinden R, Ruecker A, Wickham KS, Rochford R, Gahagen J, Iyer L, Riccio E, Mirsalis J,
507 Bathhurst I, Rueckle T, Ding X, Campo B, Leroy D, Rogers MJ, et al. 2015. A long-
508 duration dihydroorotate dehydrogenase inhibitor (DSM265) for prevention and treatment
509 of malaria. Science Trans Med 7:296ra111.
510 17. Phillips MA, Gujjar R, Malmquist NA, White J, El Mazouni F, Baldwin J, Rathod PK.
511 2008. Triazolopyrimidine-based dihydroorotate dehydrogenase inhibitors with potent and
512 selective activity against the malaria parasite *Plasmodium falciparum*. J Med Chem.
513 18. Baldwin J, Michnoff CH, Malmquist NA, White J, Roth MG, Rathod PK, Phillips MA.
514 2005. High-throughput screening for potent and selective inhibitors of *Plasmodium*
515 *falciparum* dihydroorotate dehydrogenase. J Biol Chem 280:21847-21853.
516 19. Nilsen A, LaCrue AN, White KL, Forquer IP, Cross RM, Marfurt J, Mather MW, Delves
517 MJ, Shackleford DM, Saenz FE, Morrisey JM, Steuten J, Mutka T, Li Y, Wirjanata G,

518 Ryan E, Duffy S, Kelly JX, Sebayang BF, Zeeman AM, Noviyanti R, Sinden RE, Kocken
519 CH, Price RN, Avery VM, Angulo-Barturen I, Jimenez-Diaz MB, Ferrer S, Herreros E,
520 Sanz LM, Gamo FJ, Bathurst I, Burrows JN, Siegl P, Guy RK, Winter RW, Vaidya AB,
521 Charman SA, Kyle DE, Manetsch R, Riscoe MK. 2013. Quinolone-3-diarylethers: a new
522 class of antimalarial drug. Sci Transl Med 5:177ra37.
523 20. Winter RW, Kelly JX, Smilkstein MJ, Dodean R, Bagby GC, Rathbun RK, Levin JI,
524 Hinrichs D, Riscoe MK. 2006. Evaluation and lead optimization of anti-malarial acridones.
525 Exp Parasitol 114:47-56.
526 21. Smilkstein MJ, Forquer I, Kanazawa A, Kelly JX, Winter RW, Hinrichs DJ, Kramer DM,
527 Riscoe MK. 2008. A drug-selected *Plasmodium falciparum* lacking the need for
528 conventional electron transport. Molec Biochem Parasitol 159:64-68.
529 22. Stickles AM, De Almeida MJ, Morrisey JM, Sheridan KA, Forquer IP, Nilsen A, Winter
530 RW, Burrows JN, Fidock DA, Vaidya AB, Riscoe MK. 2015. Subtle changes in endochin-
531 like quinolone structure alter the site of inhibition within the cytochrome *bc 1* complex of
532 *Plasmodium falciparum*. Antimicrob Agents Chemother 59:1977-1982.
533 23. Mandt REK, Lafuente-Monasterio MJ, Sakata-Kato T, Luth MR, Segura D, Pablos-
534 Tanarro A, Viera S, Magan N, Ottilie S, Winzeler EA, Lukens AK, Gamo FJ, Wirth DF.
535 2019. In vitro selection predicts malaria parasite resistance to dihydroorotate
536 dehydrogenase inhibitors in a mouse infection model. Sci Transl Med 11.
537 24. Ke H, Morrisey JM, Ganesan SM, Painter HJ, Mather MW, Vaidya AB. 2011. Variation
538 among *Plasmodium falciparum* strains in their reliance on mitochondrial electron transport
539 chain function. Eukaryotic Cell 10:1053-61.
540 25. Ganesan SM, Morrisey JM, Ke H, Painter HJ, Laroiya K, Phillips MA, Rathod PK, Mather
541 MW, Vaidya AB. 2011. Yeast dihydroorotate dehydrogenase as a new selectable marker
542 for *Plasmodium falciparum* transfection. Molec Biochem Parasitol 177:29-34.
543 26. Vincent IM, Barrett MP. 2015. Metabolomic-based strategies for anti-parasite drug
544 discovery. J Biomol Screen 20:44-55.
545 27. Creek DJ, Barrett MP. 2014. Determination of antiprotozoal drug mechanisms by
546 metabolomics approaches. Parasitol 141:83-92.
547 28. Ross LS, Gamo FJ, Lafuente-Monasterio MJ, Singh OM, Rowland P, Wiegand RC, Wirth
548 DF. 2014. In vitro resistance selections for *Plasmodium falciparum* dihydroorotate
549 dehydrogenase inhibitors give mutants with multiple point mutations in the drug-binding
550 site and altered growth. J Biol Chem 289:17980-95.
551 29. Srivastava IK, Morrisey JM, Darrouzet E, Daldal F, Vaidya AB. 1999. Resistance
552 mutations reveal the atovaquone-binding domain of cytochrome *b* in malaria parasites. Mol
553 Microbiol 33:704-11.
554 30. Bedingfield PTP, Cowen D, Acklam P, Cunningham F, Parsons MR, McConkey GA,
555 Fishwick CWG, Johnson AP. 2012. Factors Influencing the specificity of inhibitor binding
556 to the human and malaria parasite dihydroorotate dehydrogenases. J Med Chem 55:5841-
557 5850.

558 31. Munier-Lehmann H, Vidalain PO, Tangy F, Janin YL. 2013. On dihydroorotate
559 dehydrogenases and their inhibitors and uses. J Med Chem 56:3148-67.
560 32. Patel V, Booker M, Kramer M, Ross L, Celatka CA, Kennedy LM, Dvorin JD, Duraisingh
561 MT, Sliz P, Wirth DF, Clardy J. 2008. Identification and characterization of small molecule
562 inhibitors of *Plasmodium falciparum* dihydroorotate dehydrogenase. J Biol Chem
563 283:35078-35085.
564 33. Wells TNC, Van Huijsduijnen RH, Van Voorhis WC. 2015. Malaria medicines: a glass
565 half full? Nat Rev Drug Discov 14:424-442.
566 34. Ghorbal M, Gorman M, Macpherson CR, Martins RM, Scherf A, Lopez-Rubio J-J. 2014.
567 Genome editing in the human malaria parasite *Plasmodium falciparum* using the CRISPR-
568 Cas9 system. Nat Biotech 32:819-821.
569 35. Goodman CD, Siregar JE, Mollard V, Vega-Rodriguez J, Syafruddin D, Matsuoka H,
570 Matsuzaki M, Toyama T, Sturm A, Cozijnsen A, Jacobs-Lorena M, Kita K, Marzuki S,
571 McFadden GI. 2016. Parasites resistant to the antimalarial atovaquone fail to transmit by
572 mosquitoes. Science 352:349-53.
573 36. Bajzikova M, Kovarova J, Coelho AR, Boukalova S, Oh S, Rohlenova K, Svec D,
574 Hubackova S, Endaya B, Judasova K, Bezawork-Geleta A, Kluckova K, Chatre L,
575 Zobalova R, Novakova A, Vanova K, Ezrova Z, Maghzal GJ, Magalhaes Novais S,
576 Olsinova M, Krobova L, An YJ, Davidova E, Nahacka Z, Sobol M, Cunha-Oliveira T,
577 Sandoval-Acuña C, Strnad H, Zhang T, Huynh T, Serafim TL, Hozak P, Sardao VA,
578 Koopman WJH, Ricchetti M, Oliveira PJ, Kolar F, Kubista M, Truksa J, Dvorakova-
579 Hortova K, Pacak K, Gurlich R, Stocker R, Zhou Y, Berridge MV, Park S, Dong L,
580 Rohlena J, Neuzil J. 2019. Reactivation of dihydroorotate dehydrogenase-driven
581 pyrimidine biosynthesis restores tumor growth of respiration-deficient cancer cells. Cell
582 Metabol 29:399-416.e10.
583 37. Trager W, Jensen JB. 1976. Human malaria parasites in continuous culture. Science
584 193:673-5.
585 38. Lambros C, Vanderberg JP. 1979. Synchronization of *Plasmodium falciparum* erythrocytic
586 stages in culture. J Parasitol 65:418-20.
587 39. Desjardins RE, Canfield CJ, Haynes JD, Chulay JD. 1979. Quantitative assessment of
588 antimalarial activity in vitro by a semiautomated microdilution technique. Antimicrob
589 Agents Chemother 16:710-718.
590 40. Smilkstein M, Sriwilaijaroen N, Kelly JX, Wilairat P, Riscoe M. 2004. Simple and
591 inexpensive fluorescence-based technique for high-throughput antimalarial drug screening.
592 Antimicrob Agents Chemother 48:1803-6.
593 41. Haynes JD, Moch JK. 2002. Automated synchronization of *Plasmodium falciparum*
594 parasites by culture in a temperature-cycling incubator. Methods Molec Med 72:489-497.
595 42. Mather MW, Morrisey JM, Vaidya AB. 2010. Hemozoin-free *Plasmodium falciparum*
596 mitochondria for physiological and drug susceptibility studies. Mol Biochem Parasitol
597 174:150-3.

598 43. Olszewski KL, Llinas M. 2013. Extraction of hydrophilic metabolites from *Plasmodium*
599 *falciparum*-infected erythrocytes for metabolomic analysis. Methods Molec Biol 923:259-
600 66.
601 44. Cobbold SA, Chua HH, Nijagal B, Creek DJ, Ralph SA, McConville MJ. 2015. Metabolic
602 dysregulation induced in *Plasmodium falciparum* by dihydroartemisinin and other front
603 line antimalarial drugs. J Infect Dis doi:10.1093/infdis/jiv372.
604 45. Lu W, Clasquin MF, Melamud E, Amador-Noguez D, Caudy AA, Rabinowitz JD. 2010.
605 Metabolomic analysis via reversed-phase ion-pairing liquid chromatography coupled to a
606 stand alone orbitrap mass spectrometer. Anal Chem 82:3212-21.
607 46. Pulcini S, Staines HM, Lee AH, Shafik SH, Bouyer G, Moore CM, Daley DA, Hoke MJ,
608 Altenhofen LM, Painter HJ, Mu J, Ferguson DJ, Llinas M, Martin RE, Fidock DA, Cooper
609 RA, Krishna S. 2015. Mutations in the *Plasmodium falciparum* chloroquine resistance
610 transporter, PfCRT, enlarge the parasite's food vacuole and alter drug sensitivities. Sci Rep
611 5:14552.
612 47. Goecks J, Nekrutenko A, Taylor J, Galaxy T. 2010. Galaxy: a comprehensive approach for
613 supporting accessible, reproducible, and transparent computational research in the life
614 sciences. Genome Biol 11:R86.
615 48. Li H, Durbin R. 2009. Fast and accurate short read alignment with Burrows-Wheeler
616 transform. Bioinformatics 25:1754-60.
617 49. DePristo MA, Banks E, Poplin R, Garimella KV, Maguire JR, Hartl C, Philippakis AA,
618 del Angel G, Rivas MA, Hanna M, McKenna A, Fennell TJ, Kernytsky AM, Sivachenko
619 AY, Cibulskis K, Gabriel SB, Altshuler D, Daly MJ. 2011. A framework for variation
620 discovery and genotyping using next-generation DNA sequencing data. Nat Gen 43:491-
621 8.
622 50. Garrison E, Marth G. 2012. Haplotype-based variant detection from short-read sequencing.
623 arXiv:12073907 [q-bioGN].
624 51. Cingolani P, Platts A, Wang le L, Coon M, Nguyen T, Wang L, Land SJ, Lu X, Ruden
625 DM. 2012. A program for annotating and predicting the effects of single nucleotide
626 polymorphisms, SnpEff: SNPs in the genome of *Drosophila melanogaster* strain w1118;
627 iso-2; iso-3. Fly (Austin) 6:80-92.
628 52. Abyzov A, Urban AE, Snyder M, Gerstein M. 2011. CNVnator: an approach to discover,
629 genotype, and characterize typical and atypical CNVs from family and population genome
630 sequencing. Genome Res 21:974-84.
631 53. Nkrumah LJ, Muhle RA, Moura PA, Ghosh P, Hatfull GF, Jacobs WR, Jr., Fidock DA.
632 2006. Efficient site-specific integration in *Plasmodium falciparum* chromosomes mediated
633 by mycobacteriophage Bxb1 integrase. Nat Methods 3:615-21.
634 54. Fidock DA, Wellems TE. 1997. Transformation with human dihydrofolate reductase
635 renders malaria parasites insensitive to WR99210 but does not affect the intrinsic activity
636 of proguanil. PNAS 94:10931-10936.

637 55. van den Hoff MJ MA, and Lamers WH. 1992. Electroporation in 'intracellular' buffer
638 increases cell survival. Nucleic Acid Res 20:2902.

639

640

641 **Figure Legends:**

642 **Figure 1: Drug-resistant phenotyping of *P.f.* strain SB1-A6.** A) Early ring-stage *P. falciparum*
643 strain D6 (blue) and SB1-A6 (red) were exposed to titrating concentrations of atovaquone or DSM-
644 1. Their susceptibility was directly compared to a phenocopy strain, D10:yDHODH (grey, red
645 outline) and its parent, D10 (grey, blue outline). Parasite survival was determined using a
646 traditional 48-h SYBR-green growth inhibition assay and plotted as an average of three technical
647 replicates (±SD). B) Reversal of the SB1-A6 phenotype is demonstrated by exposure of ring-stage
648 parasites to titrating concentrations of atovaquone with (red circles, dashed line) or without the
649 addition of 1.0 μM proguanil (red circles, solid line). Parasite survival was determined as in (A).
650 C) Whole-cell metabolomic analysis was performed on trophozoite stages of both *P.f.* strain D6
651 and SB1-A6 after two hours of 10x $1C_{50}$ exposure to either atovaquone or DSM-1. Metabolic
652 changes are displayed as a MetaPrint profile (8) and highlighted are the increasing (blue outline)
653 metabolites in D6 compared to no change SB1-A6 (red outline). D) The increased metabolites
654 highlighted (C) in *P.f.* strain D6 (blue) are plotted as absolute signal determined by the average
655 total ion counts (biological duplicates in technical triplicate) for *N*-carbamoyl-L-aspartate and
656 dihydroorotate in the presence of atovaquone (10nM), DSM-1 (1.5 μM) or absence of drug relative
657 to *P.f.* strain SB1-A6 (red).

658

659 **Figure 2: Genetic and molecular differences in *P.f.* strain SB1-A6.** A) Whole-genome
660 sequencing revealed a point mutation in PF3D7_0603300 (*pfdhodh*) and this mutation was verified
661 by Sanger sequencing. A trace of the PfDHODH coding sequence is shown from nucleotide 818-
662 836 and the single nucleotide polymorphism change from the parental D6 to SB1-A6 at nucleotide
663 G827T (yellow highlight) which results in the amino acid change C276F. Additionally, WGS

664 revealed B) a 1.9x copy number increase of a ~20kb region (red highlight) on chromosome 6 which
665 includes PF3D7_0603300 (*pfdhodh*). Copy number increase was calculated and graphically
666 represented using Intansiv (v. 0.99.3). C) Structural comparisons of wild-type (PDB 4RX0, light
667 grey, C276 highlighted in blue) and mutant (PDB 6E0B, dark grey, C276F highlighted in red)
668 PfDHODH bound with FMN, as well as the merged structure surrounding amino acid 276 (inset;
669 cysteine in blue and phenylalanine in red, represent the isosurface of each sidechain) were made
670 using PyMOL 2.3.4. D) Western blot analysis of the PfDHODH expression in both D6 and SB1-
671 A6 probed with anti-mouse PfDHODH antibody (1:300) compared to *Pf*Aldolase (anti-mouse
672 *Pf*Aldolase-HRP, 1:5000) as a loading control. E) Percent inhibition of PfDHODH activity and
673 F) capture of total PfDHODH activity in isolated mitochondria from SB1-A6 (red) and D6 (blue)
674 in the presence of titrating concentrations of DSM-1.

675

676 **Figure 3: Phenotyping Individual Genetic Contributions to *P.f.* SB1-A6 Resistance.** A)
677 Strategy for phenotyping a mimic of the PfDHODH genotype in the wild-type *P.f.* D6 strain.
678 Episomal expression of an additional copy of wild-type PfDHODH (blue) aims to genocopy a
679 CNV and episomal expression of the mutant PfDHODH (red) genocopies a CNV of the mutation
680 to capture the contribution of these genotypes to the resistance phenotype. B) These transgenic
681 lines, D6::wtDHODH (blue triangle, dashed) and D6::mutDHODH (red open circle, dashed), were
682 assessed for their susceptibility to titrating concentrations of both atovaquone and DSM-1 in
683 comparison to the parental strains, A6 (red solid triangle) and D6 (blue solid square). Parasite
684 survival was determined using a traditional 48-h SYBR-green growth inhibition assay and plotted
685 as an average of three technical replicates (±SD). C) Graphic representation of the CRISPR/Cas9-
686 mediated mutational strategy for modification of PfDHODH in both the wild-type D6 and mutant

687 strain SB1-A6. A plasmid expressing Cas9 was cotransfected with a plasmid that contains the
688 DHODH repair template that encodes for C276 (wild-type) or F276 (mutant) that are provided to
689 introduce a single point mutation converting strain D6 to C276F and SB1-A6 to F276C,
690 respectively. The CRISPR/Cas9 mutated strains $D6^{C276F}$ (blue solid diamond, dashed) and SB1-
691 $A6^{F276C}$ (red solid triangle, dashed) were then assayed for their susceptibility to titrating
692 concentrations of both atovaquone and DSM-1 in comparison to the parental strains, A6 (red solid
693 triangle) and D6 (blue solid square). Parasite survival was determined using a traditional 48-h
694 SYBR-green growth inhibition assay and plotted as an average of three technical replicates (±SD).

**Figure 1**

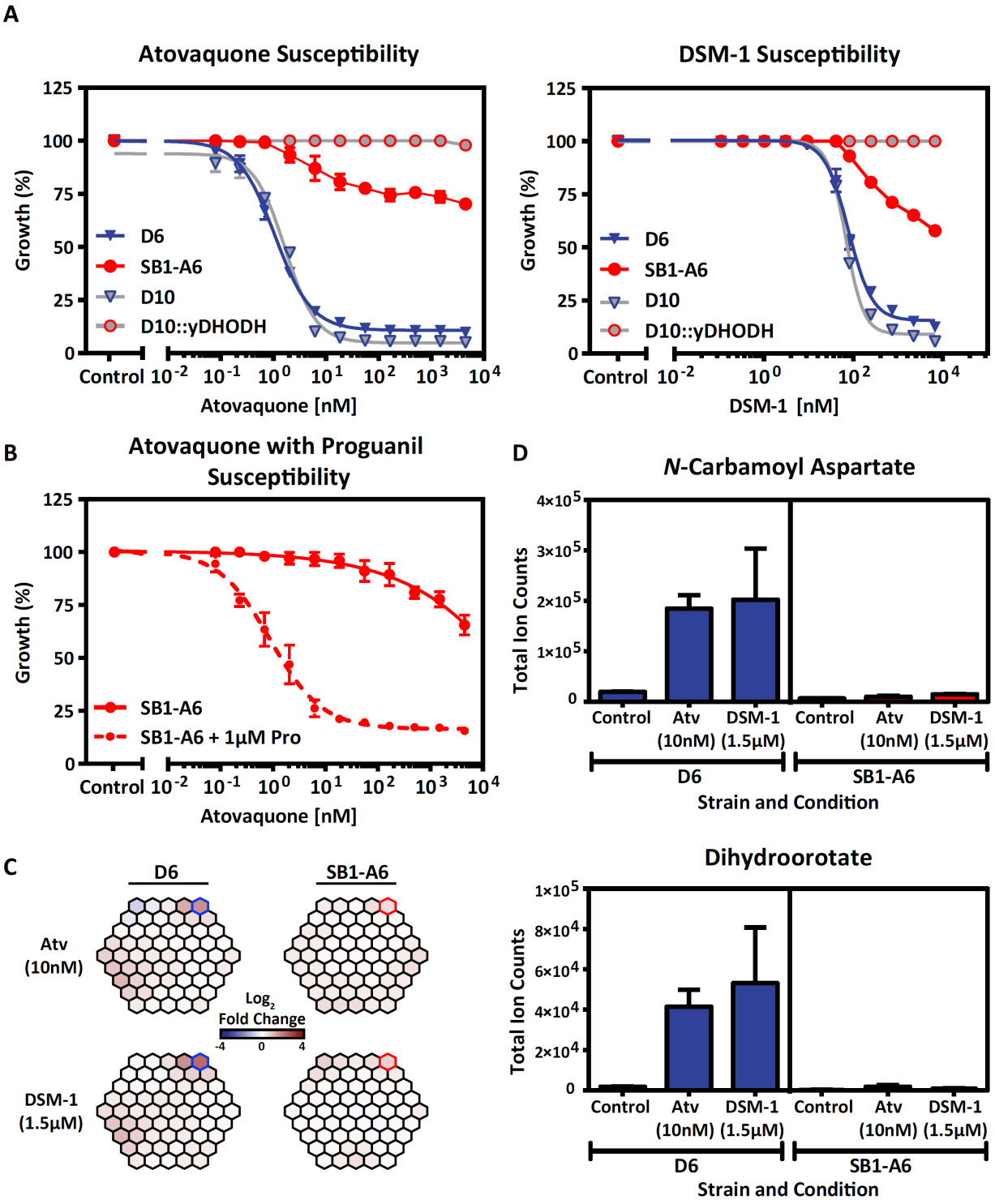
A
Atovaquone Susceptibility
Growth (%)
125
100
75
50
25
0
D6
SB1-A6
D10
D10::yDHODH
Control
$10^{-2}$
$10^{-1}$
$10^{0}$
$10^{1}$
$10^{2}$
$10^{3}$
$10^{4}$
Atovaquone [nM]
DSM-1 Susceptibility
DSM-1 [nM]
B
Atovaquone with Proguanil Susceptibility
SB1-A6
SB1-A6 + 1µM Pro
C
D6
SB1-A6
Atv (10nM)
DSM-1 (1.5µM)
$Log_2$ Fold Change
-4
0
4
D
*N*-Carbamoyl Aspartate
Total Ion Counts
$4\times10^5$
$3\times10^5$
$2\times10^5$
$1\times10^5$
Control
Atv (10nM)
DSM-1 (1.5µM)
D6
SB1-A6
Strain and Condition
Dihydroorotate
$1\times10^5$
$8\times10^4$
$6\times10^4$
$4\times10^4$
$2\times10^4$

**Figure 2**

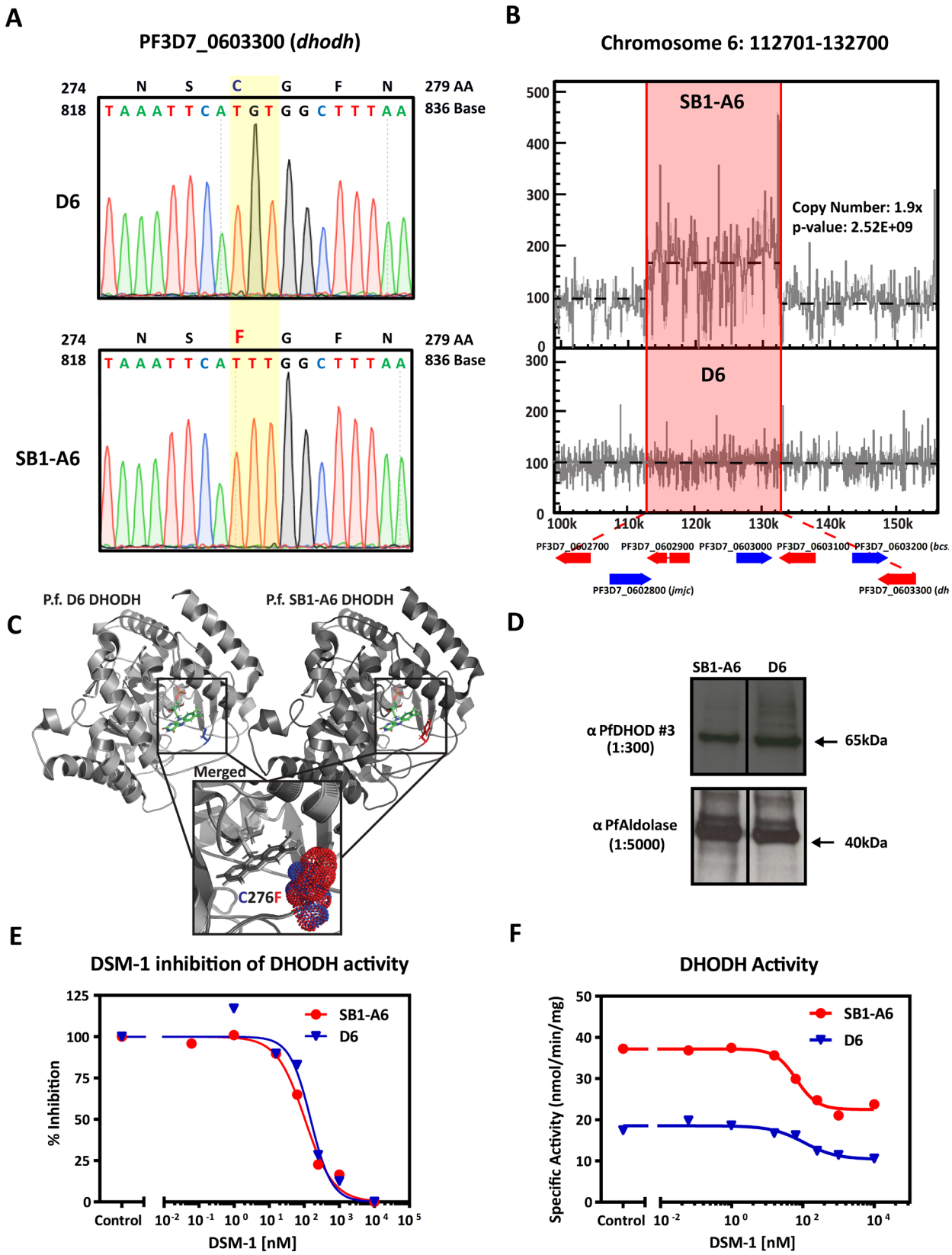
A
PF3D7_0603300 (dhodh)
274 N S C G F N 279 AA
818 T A A A T T C A T G T G G C T T T A A 836 Base
D6
274 N S F G F N 279 AA
818 T A A A T T C A T T T G G C T T T A A 836 Base
SB1-A6
B
Chromosome 6: 112701-132700
SB1-A6
Copy Number: 1.9x
p-value: 2.52E+09
D6
100k 110k 120k 130k 140k 150k
PF3D7_0602700 PF3D7_0602900 PF3D7_0603000 PF3D7_0603100 PF3D7_0603200 (bcs
PF3D7_0602800 (jmjc)
PF3D7_0603300 (dh
C
P.f. D6 DHODH
P.f. SB1-A6 DHODH
Merged
C276F
D
SB1-A6 D6
α PfDHOD #3 (1:300)
65kDa
α PfAldolase (1:5000)
40kDa
E
DSM-1 inhibition of DHODH activity
% Inhibition
SB1-A6
D6
Control
DSM-1 [nM]
F
DHODH Activity
Specific Activity (nmol/min/mg)
SB1-A6
D6
Control
DSM-1 [nM]

697

## Figure 3

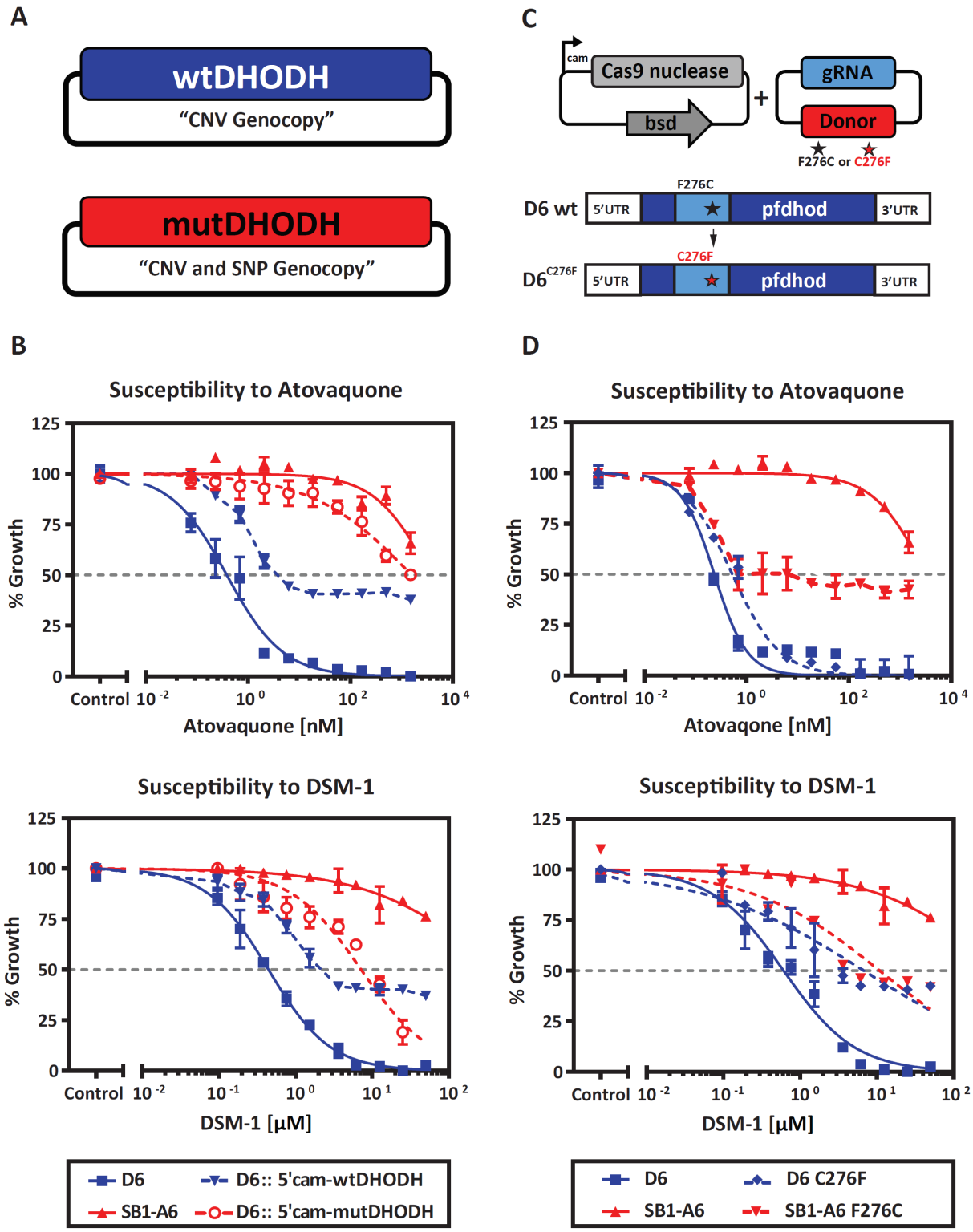
A
wtDHODH
"CNV Genocopy"
mutDHODH
"CNV and SNP Genocopy"
C
cam
Cas9 nuclease
bsd
+
gRNA
Donor
F276C or C276F
D6 wt
5'UTR
F276C
pfdhod
3'UTR
D6C276F
5'UTR
C276F
pfdhod
3'UTR
B
Susceptibility to Atovaquone
% Growth
Atovaquone [nM]
Control
Susceptibility to DSM-1
DSM-1 [µM]
D6
D6:: 5'cam-wtDHODH
SB1-A6
D6:: 5'cam-mutDHODH
D
Susceptibility to Atovaqone
Atovaqone [nM]
Susceptibility to DSM-1
DSM-1 [µM]
D6
D6 C276F
SB1-A6
SB1-A6 F276C